European Journal of Radiology 115 (2019) 53–58

Contents lists available at ScienceDirect

European Journal of Radiology

journal homepage: www.elsevier.com/locate/ejrad

Research article

Magnetic resonance cholangiopancreatography at 3 Tesla: Image quality comparison between 3D compressed sensing and 2D single-shot acquisitions

Fabian K. Lohöfer[a,1], Georgios A. Kaissis[a,1], Michael Rasper[a], Christoph Katemann[b], Andreas Hock[b], Johannes M. Peeters[c], Christoph Schlag[d], Ernst J. Rummeny[a], Dimitrios Karampinos[a], Rickmer F. Braren[a,*]

[a] Institute for Diagnostic and Interventional Radiology, Faculty of Medicine of the Technical University Munich, Ismaninger Straße 22, D-81675 Munich, Germany
[b] Philips Healthcare, Hamburg, Germany
[c] Philips Healthcare, Best, Netherlands
[d] II. Medical Department, Faculty of Medicine of the Technical University Munich, Ismaninger Straße 22, D-81675 Munich, Germany

ARTICLE INFO

Keywords:
Diagnostic techniques and procedures
Magnetic resonance imaging
Magnetic resonance cholangiopancreatography
Biliary tract
Pancreatic ducts

ABSTRACT

Objectives: To compare the image quality between compressed sensing (CS) 3D-magnetic resonance cholangiopancreatography (MRCP) using respiratory-triggered (RT) and breath-hold (BH) acquisitions and 2D single-shot breath-hold (SSBH) MRCP at 3 T MRI.

Methods: 53 datasets were retrospectively assessed. 3D-MRCP with CS (RT-CS10, BH-CS24) and 2D-SSBH MRCP were acquired. Overall image quality, blurring/motion artifacts and discernibility of the pancreaticobiliary tree (PBT) structures were scored on a 4-point scale by 2 radiologists. The contrast ratio between the common bile duct and its adjacent tissue was measured by region-of-interest (ROI) analysis. Signal intensity increase at the boundaries of the ducts was quantified by *line profiles* to objectively characterize blurring and motion artifacts.

Results: Total scan duration was 17 s for BH-CS24, 1m12 s for 2D-SSBH and 3m48 s for RT-CS10. Images acquired with CS were consistently rated superior in terms of image quality, background suppression, blurring and discernibility of PBT structures compared to 2D-SSBH images. RT-CS10 was superior to BH-CS24 for all ratings except for blurring. Objective analysis yielded the highest contrast ratio for RT-CS10 (0.91 ± 0.04) followed by BH-C24 (0.88 ± 0.05) and 2D-SSBH (0.85 ± 0.06); *one-way ANOVA* $P < 0.0001$. The *line-profile* slope through the CBD was significantly higher in BH-CS24 (37.91 ± 6.38% of maximum intensity/mm) compared to RT-CS10 (29.46 ± 8.17% of maximum intensity/mm) and on par with 2D-SSBH (35.8 ± 12.30% of maximum intensity/mm); *one-way-ANOVA* $P = 0.017$.

Conclusion: CS allows acquisition of volumetric image data with improved image quality compared to SSBH. CS24 yields substantial gains in acquisition speed while robust towards artifacts, enabling diagnostic image quality with a single breath-hold acquisition.

1. Introduction

Magnetic resonance cholangiopancreatography (MRCP) is the gold-standard method for non-invasive, contrast-media free assessment of the pancreaticobiliary tree [1,2]. In light of long acquisition times and often poor image quality of respiratory-triggered 3D MRCP sequences, single-shot breath-hold 2D sequences are still commonly applied. However, the utility of this type of sequence is limited mainly due to overlap of unsuppressed anatomical structures and no option for multiplanar reconstructions [3,4]. Parallel imaging techniques such as sensitivity encoding (SENSE) can accelerate MRI acquisition at the cost of reduced signal-to-noise ratio [5]. Compressed sensing, the random undersampling of *k*-space combined with an iterative image reconstruction process, is another acceleration technique which exploits e.g. image domain sparsity as seen in heavily T2w MRCP imaging data [6]. The two methods can be combined synergistically to further

Abbreviations: BH, breath-hold; CBD, common bile duct; CS, compressed sensing; MPR, multiplanar reformations; MRCP, magnetic resonance cholangiopancreatography; MRI, magnetic resonance imaging; PBT, pancreaticobiliary tree; ROI, region-of-interest; RT, respiratory-triggered; SENSE, sensitivity encoding; SNR, signal to noise ratio; SSBH, single-shot breath-hold; TSE, Turbo spin echo

* Corresponding author.
E-mail address: rbraren@tum.de (R.F. Braren).

[1] These authors contributed equally to this work and share the first authorship.

https://doi.org/10.1016/j.ejrad.2019.04.002
Received 13 February 2019; Received in revised form 28 March 2019; Accepted 2 April 2019

decrease acquisition times [7,8]. Thus, high acceleration rates have enabled the acquisition of respiratory/navigator-triggered [9–12] and even single breath-hold [13,14] 3D MRCP datasets with sufficient SNR and gains in diagnostic image quality. CS is generally considered beneficial for accelerating 3D TSE MRCP scans and recent publications recommends CS accelerated MRCP as the preferred sequence for imaging the pancreaticobiliary system in terms of image quality and acquisition time at 1.5 and 3 T [9,14]. However, there is a paucity of literature regarding the question whether CS accelerated MRCP should be performed as a respiratory-triggered sequence or as a breath-hold sequence. In patients with irregular breathing pattern, and thus potential malfunction of the respiratory triggering, or patients with limited endurance to lengthy examinations, CS accelerated breath-hold MRCP can be of major advantage [12]. We therefore aimed to elucidate the advantages of this acquisition by comparing subjective and objective metrics of image quality between a breath-hold single-shot 2D MRCP, and two 3D MRCP sequences (breath-hold and respiratory-triggered) with an optimized integrated compressed sensing and parallel imaging technique on a latest-generation clinical 3 T MRI system.

2. Material and methods

Approval by the institutional ethics committee (180/17S, Ethikkommission der Fakultät für Medizin der Technischen Universität München) was received for the study. The requirement to obtain written informed consent for retrospective data analysis was waived. All analyses were carried out in compliance with the pertinent regulations and requirements.

2.1. Patient cohort

We considered 80 datasets of patients who underwent routine clinical MRCP examination from the time of installation of the MRI system (February 2018) until June 2018 for inclusion in the study. Datasets of patients who did not receive all MRCP sequences as detailed below (N = 27) were excluded. The final patient cohort consisted of 53 patients, 26 males and 27 females. Average patient age was 58.3 ± 17.0 years (range 18–85 years). MRCP was performed with the following indications: evaluation of focal pancreatic lesions (n = 26), pancreatitis (n = 8), evaluation of biliary lesions (n = 14) and post-operative follow up for pancreatic or biliary disease (n = 5).

2.2. MRCP image acquisition

A 2-dimensional single-shot breath-hold (8 s time per projection in expiration) MRCP (2D-SSBH) with 9 projections across the pancreatobiliary tree (PBT) and two 3-dimensional MRCP sequences (a respiratory-triggered, compressed sensing 3D MRCP utilizing a *CS factor* of 10 (*RT-CS10*) and a breath-hold, compressed sensing 3D-MRCP utilizing a *CS factor* of 24 (*BH-CS24*)) were acquired on a 3 T MRI scanner (*Philips Ingenia Elition X; Philips Medical Systems*, Best, The Netherlands). The relevant technical scan parameters are listed in Table 1.

The CS technique used in the present work was based on the combination of SENSE and CS, labelled as Compressed SENSE or C-SENSE. The employed technique used the coil sensitivity information from a SENSE calibration scan and randomly undersamples both the central and outer part of *k*-space, following a smooth sampling density as moving from the center to outer parts of k-space. The acquisition and reconstruction were based on the vendor's implementation (Compressed SENSE, Philips Healthcare). A single CS acceleration factor was defined for the two CS MRCP sequence variants and the sampled k-space pattern (central and outer part) was defined based on the vendor's implementation. In order to maintain a balance between noise reduction and data consistency for CS, an iterative L1-minimization reconstruction technique, forcing data fidelity, and image sparsity in the wavelet domain was used.

The following sequences were also acquired under the standard clinical protocol: axial and coronal 3 mm T2w, axial 4 mm diffusion-weighted imaging and 4 mm mDIXON dynamic. These sequences were not utilized in the present data analysis.

2.3. Quantitative image analysis

For contrast ratio analysis, a 5 mm region of interest (ROI) was manually drawn at a distance 5 mm distal to the bifurcation of the hepatic ducts in the common bile duct (CBD) in coronal MRCP images. Another 5 mm ROI was drawn in the adjacent periductal tissue, avoiding areas with motion artifacts.

The contrast ratio was calculated using the following formula:

$$Contrast\ ratio = (SI_{CBD} - SI_{periductal\ tissue})/(SI_{CBD} + SI_{periductal\ tissue})$$

SI: ROI average signal intensity; CBD: common bile duct

For objective quantification of blurring and motion artifacts, a *line profile* perpendicular to the common bile duct 5 mm distal to the hepatic duct bifurcation was generated using FIJI's [15] "Line Profile" function. To enable comparison between different sequences, signal intensities along the line profile were expressed as percentages of the peak intensity inside the CBD. The maximum line profile slope was reported as percentage change per mm at the boundary of the duct.

2.4. Qualitative image analysis

All images were assessed by two radiologists with 7 years (M.R.) and 6 years (F.L.) of experience. For CS, images were provided as 3 plane multiplanar reformations (MPR) from RT-CS10 (0.79 mm slice thickness) and BH-CS24 (1.00 mm slice thickness), sliced maximum intensity projection (MIP) (slice thickness/increment 6/3 mm) and 3D-surface-renderings from MIP. For 2D-SSBH, 9 *thick slab* (4 cm) projections, radially arranged around the pancreatic head, were provided.

Images were viewed under radiological reporting room conditions on certified monitors and observers were allowed to adjust window level and width ad libitum.

The images of the three different sequences were assessed in separate sessions with an interval of two weeks. Observers were blinded to the dataset name.

Qualitative analysis was performed using a 4-point *Likert* scale. **Overall image quality** was rated as *1 = poor; 2 = fair; 3 = good; 4 = excellent*. **Blurring and motion artifacts** were rated as *1 = image not diagnostic because of artifacts; 2 = major artifacts; 3 = minor artifacts; 4 = no artifacts*. **Background suppression** was rated as *1 = significant background signal, which hampers diagnostic capability score; 2 = substantial background signal with significant image quality degradation; 3 = noticeable background signal but with only mild image quality degradation; 4 = sufficient background suppression without degrading image quality*. **Visualization of the biliary and pancreatic duct structures** was rated as *1 = detection of ductal structures almost impossible; 2 = ductal structures partially visible; 3 = most of the ductal structures visualized; 4 = perfect visualization of the entire ductal structure*.

2.5. Statistical analysis

Variables were tested for normal distribution using the *D'Agostino-Pearson omnibus K2 test*. *Student's t*-test was used for mean comparisons of normally distributed variables. *One-way ANOVA* and *Tukey´s test* was used for multiple comparisons. The *Kruskal-Wallis-method* was used for ANOVA of nonparametric data. Inter-observer agreement was calculated using *Cohen´s kappa*. Multiple testing-correction was performed where necessary.

All statistics were performed using *Prism* Version 7 (*GraphPad Software*) and *IBM SPSS* Version 25.

A two-tailed P-value below 0.05 was considered statistically

Table 1
Scan parameters of the three MRCP sequences.

	2D-SSBH	RT-CS10	BH-CS-24
Gating	Breath-hold	Respiratory-triggered	Breath-hold
CS acceleration factor	1	10	24
Acquisition time (s)	1:12 (9 BHs of 8 s)	3:48	17.5
FOV (mm) FH; RL; AP	300; 300; -	280; 280; 95.3	260; 290.8; 80
Acquisition voxel size (mm) FH/ RL/AP	0.94/1.17/40.0 (slice thickness)	1.10/1.10/1.10	1.00/1.00/2.00
Reconstruction voxel size (mm) FH/RL/AP	0.59/0.59/40	0.73/0.73/0.79	0.55/.055/1
Fast imaging mode	TSE	TSE	TSE
TE_{eff} /TE_{equiv} (ms)	–	480 / 427	584 /445
Act. TR (ms)	8000	1418	2500
Act. TE (ms)	740	480	584
Flip angle (°)	90	90	80
Fat suppression	SPAIR	SPIR	SPIR
Receiver bandwidth (Hz/pixel)	407	236	364
TSE factor	256	90	180

significant.

3. Results

3.1. Qualitative image analysis

3.1.1. Overall image quality is significantly superior in CS compared to SSBH

The mean observer rating for overall image quality and contrast of the pancreaticobiliary tree was significantly higher for RT-CS10 (2.92 ± 0.60) and BH-CS24 (2.91 ± 0.68) compared to 2D-SSBH (2.57 ± 0.65); one-way *ANOVA* $P < 0.0001$. No significant difference was found between the two CS acquisitions. Inter-reader agreement (*Cohen's Kappa)* for RT-CS10 was 0.86, for BH-CS24 0.88 and for 2D-SSBH 0.87. Poor overall image quality (rating: 1) was seen in 4.71% of the cases in 2D-SSBH acquisitions, whereas it was seen in none of the CS acquisitions. Fair overall image quality (rating: 2) was seen in 37.73% of the 2D-SSBH acquisitions, but only in 28.30% of the BH-CS24 and 21.70% of the RT-CS10 acquisitions.

3.1.2. Significantly less blurring and motion artifacts are found in CS than in SSBH

Significantly less blurring and motion artifacts were found in CS acquisitions compared to 2D-SSBH: average rating for BH-CS24 was 2.97 ± 0.56, for RT-CS10 2.80 ± 0.54 and for 2D-SSBH 2.70 ± 0.50; *one-way ANOVA* $P = 0.0002$. However, BH-CS24 significantly outperformed RT-CS10 (*paired t*-test $P = 0.02$). Inter-reader agreement (*Cohen's Kappa)* for RT-CS10 was 0.80, for BH-CS24 0.80 and for 2D-SSBH 0.84.

3.1.3. Background suppression is consistently superior in CS compared to SSBH

Background suppression of CS acquisitions was consistently rated superior to 2D-SSBH acquisition. However, only BH-CS24 reached statistical significance against 2D-SSBH. Average rating for BH-CS24 was 2.68 ± 0.63, for RT-CS10 2.57 ± 0.57 and for 2D-SSBH 2.46 ± 0.65; *one-way ANOVA* $P = 0.0006$. Inter-reader agreement (*Cohen's Kappa)* for RT-CS10 was 0.86, for BH-CS24 0.87 and for 2D-SSBH 0.90.

3.1.4. CS is superior in the visualization and image quality of the CBD, the pancreatic duct and small ductal structures of the PBT compared to 2D-SSBH

Scores for common bile duct visualization were significantly higher for RT-CS10 (3.59 ± 0.64) compared to BH-CS24 (3.44 ± 0.73) and 2D-SSBH (3.14 ± 0.80); *one-way ANOVA* $P < 0.0001$. Inter-reader agreement (*Cohen's Kappa)* for RT-CS10 was 0.80, for BH-CS24 was 0.83 and for 2D-SSBH was 0.85.

The scores for left and right hepatic duct visualization were significantly higher in BH-CS24 (left:3.50 ± 0.68; right:3.47 ± 0.68) and RT-CS10 (left:3.49 ± 0.71; right:3.57 ± 0.62) compared to 2D-SSBH (left: 3.26 ± 0.73; right: 3.34 ± 0.74; *one-way ANOVA* $P = 0.0009$ (left) and $P = 0.0113$ (right)). No significant difference was found between the two CS acquisitions in either case. Inter-reader agreement (*Cohen's Kappa)* for RT-CS10 was 0.79 (left); 0.78 (right), for BH-CS24 0.82 (left); 0.86 (right) and for 2D-SSBH 0.81 (left); 0.81 (right).

For visualization of segmental branches and the pancreatic duct, RT-CS10 was consistently awarded higher average visualization scores than BH-CS24 and 2D-SSBH. It significantly outperformed BH-CS24 in segments 5–7 and all parts of the pancreatic duct and 2D-SSBH in all segments and the proximal pancreatic duct. Regarding pancreatic duct visualization, RT-CS10 significantly outperformed BH-CS24 in all segments.

These results are summarized alongside the findings presented above in Table 2.

3.2. Quantitative image analysis

Scan duration was 17 s for BH-CS24, 1m12 s for 2D-SSBH and 3m48 s for RT-CS10.

Contrast ratio was significantly higher in RT-CS10 (0.91 ± 0.04) than in BH-CS24 (0.88 ± 0.05) and in 2D-SSBH (0.85 ± 0.06); *one-way ANOVA* $P < 0.0001$.

The *line profile* slope through the CBD was significantly higher in BH-CS24 (37.91 ± 6.38% of maximum intensity/mm) compared to RT-CS10 (29.46 ± 8.17% of maximum intensity/mm) while not differing significantly from 2D-SSBH (35.8 ± 12.30% of maximum intensity/mm, *paired t*-test $P > 0.05$); *one-way-ANOVA* $P = 0.017$.

An example case with line profiles is shown in Fig. 1.

4. Discussion

This study evaluates an optimized integrated compressed sensing and parallel imaging technique (CS) for the acquisition of 3D MRCP data sets. CS accelerated respiratory-triggered and breath-hold sequences outperform a standard thick slab single shot 2D MRCP sequence -still standard-of-care in many facilities- regarding image quality with high inter-reader agreement.

A significant drawback of the 2D-SSBH acquisitions is the presence of anatomical overlap, which can reduce diagnostic confidence and accuracy [1; 2]. (Near)-isotropic 3D acquisitions, such as the CS-based acquisitions employed in the current study enable multiplanar reconstruction, which facilitates structure and pathology delineation. Several studies have shown advantages of this technique applied to MRCP [11,14,16]. Superior image quality of CS accelerated NT 3D MRCP scans were attributed to the reduction of motion artifacts with

Table 2
Summary table of all scores for image quality parameters and visualization of the duct structures; values are shown as mean ± standard deviation. *ANOVA* P and multiple testing significance (two-tailed P < 0.05) are given. Values in bold indicate the highest value in the series. SSBH: Single-shot-breathhold, CS: compressed sense.

		2D-SSBH	RT-CS10	BH-CS24	ANOVA P	2D-SSBH vs. RT-CS10	2D-SSBH vs. BH-CS24	RT-CS10 vs BH-CS24
Overall image quality and PBT contrast		2.57 ± 0.56	**2.92 ± 0.60**	2.91 ± 0.68	< 0.0001	Sig.	Sig.	N.S.
Blurring and motion artifacts		2.70 ± 0.50	2.80 ± 0.54	**2.97 ± 0.56**	0.0002	N.S.	Sig.	Sig.
Background suppression		2.46 ± 0.65	2.57 ± 0.57	**2.68 ± 0.63**	0.0006	N.S.	Sig.	N.S.
Bile duct visualization	**Common bile duct**	3.14 ± 0.80	**3.59 ± 0.64**	3.44 ± 0.73	< 0.0001	Sig.	Sig.	Sig.
	Left hepatic duct	3.26 ± 0.73	3.49 ± 0.71	**3.50 ± 0.68**	0.0009	Sig.	Sig.	N.S.
	Right hepatic duct	3.34 ± 0.74	3.47 ± 0.68	**3.47 ± 0.62**	0.0113	Sig.	Sig.	N.S.
	Segment 2	2.25 ± 0.71	**2.48 ± 1.03**	2.32 ± 1.09	0.0206	Sig.	N.S.	N.S.
	Segment 3	2.25 ± 0.74	**2.57 ± 1.01**	2.45 ± 1.09	0.0013	Sig.	Sig.	N.S.
	Segment 4	2.14 ± 0.74	**2.62 ± 0.99**	2.48 ± 1.06	< 0.0001	Sig.	Sig.	N.S.
	Segment 5	2.34 ± 0.79	**2.69 ± 0.83**	2.49 ± 0.97	< 0.0001	Sig.	N.S.	Sig.
	Segment 6	2.32 ± 0.81	**2.66 ± 0.96**	2.36 ± 1.07	< 0.0001	Sig.	N.S.	Sig.
	Segment 7	2.31 ± 0.80	**2.68 ± 0.95**	2.38 ± 1.06	< 0.0001	Sig.	N.S.	Sig.
	Segment 8	2.39 ± 0.75	**2.72 ± 0.85**	2.58 ± 0.97	< 0.0001	Sig.	Sig.	N.S.
Pancreatic duct visualization	**Proximal**	2.97 ± 0.91	**3.21 ± 0.89**	2.77 ± 1.02	< 0.0001	Sig.	N.S.	Sig.
	Mid	2.94 ± 0.87	**2.98 ± 1.00**	2.61 ± 1.12	< 0.0001	N.S.	Sig.	Sig.
	Distal	2.54 ± 0.86	**2.69 ± 0.97**	2.19 ± 1.11	< 0.0001	N.S.	Sig.	Sig.

reduced scan times [9,13,14].

In subjective assessment of image quality, we found CS-based acquisitions and RT-CS10 in particular to outperform 2D-SSBH with high inter-reader agreement. We corroborated this finding by measuring the contrast ratio between the bile duct and its adjacent tissue, finding it to be significantly higher in RT-CS10 than in 2D-SSBH (Figs. 2 and 3).

BH-CS24 outperformed RT-CS10 regarding blurring and motion artifacts both subjectively and objectively as a result of BH-CS24 being acquired in a complete expiratory breath hold. However, RT-CS10 still provided higher artifact resistance than 2D-SSBH (Fig. 4).

If the highest possible resistance to motion blurring is desired and the patient is able to comply in performing breath-holds, our data advises the acquisition of BH-CS24 in addition to RT-CS10, which -due to the short acquisition time of 17 s- does only negligibly prolong examination times. If a dramatic reduction in scan time is desired, a singular acquisition of BH-CS24 can be considered, which yields a 72% scan time reduction compared to 2D-SSBH and a 93% reduction compared to RT-CS10 with a high chance of diagnostically sufficient image quality. These results exceed the values reported recently by Nagata et al. [17] (78% reduction in time), due to the higher SENSE factor. The optimal trade-off between image quality and acquisition duration, however, remains undetermined at this point, partly due to the fact that the exact specifications of the protocol are not published by the manufacturer. In any case, BH-CS24 scan time reduction is expected to be even more significant, due to the fact that RT-CS10 scan time varies depending on the individual breathing cycle. In cases of limited patient compliance, such as in cases of dyspnea, the higher overall performance of RT-CS10 warrants its application over 2D-SSBH despite the slightly longer examination time.

RT-CS10 was found to provide the best visualization of small ductal structures, making it particularly useful in cases such as e.g. early stages of primary sclerosing cholangitis, where small ductal structures may be

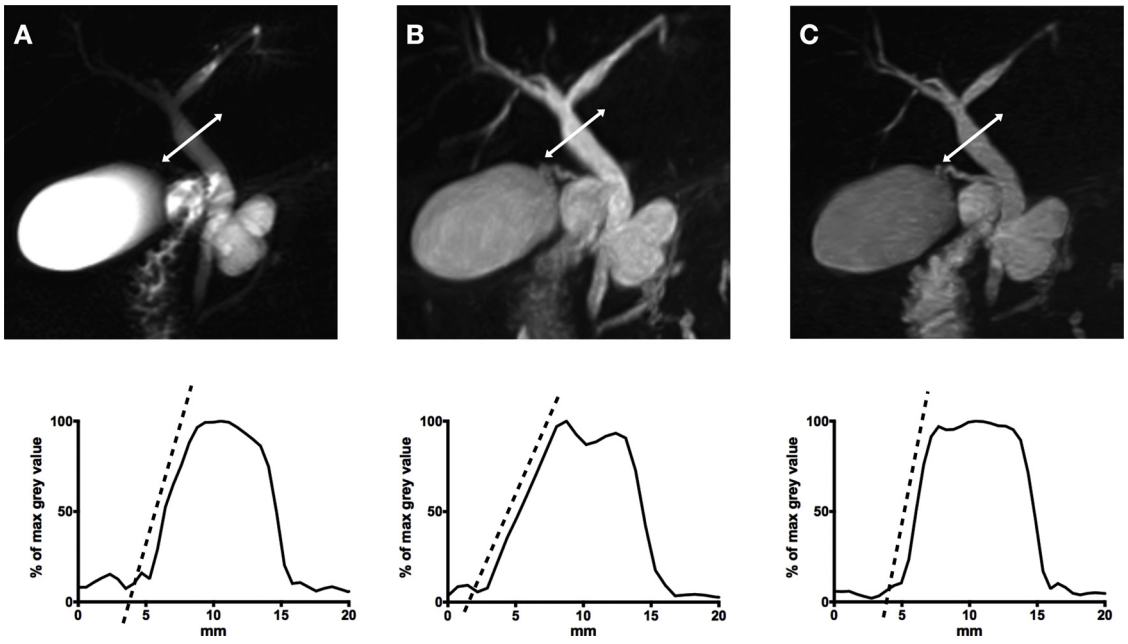

Fig. 1. Comparison of the *line profile* slope at the common bile duct in 2D-SSBH (A), RT-CS10 (B) and BH-CS24 (C). The *line profiles* were drawn through the common bile duct 5 mm distal to the bifurcation. Plots were normalized to the maximum intensity value inside the CBD. The slope is calculated by the percentage of the maximum grey value per millimeter. Slope is highest in BH-CS24 (C), followed by 2D-SSBH (A) and RT-CS10 (B).

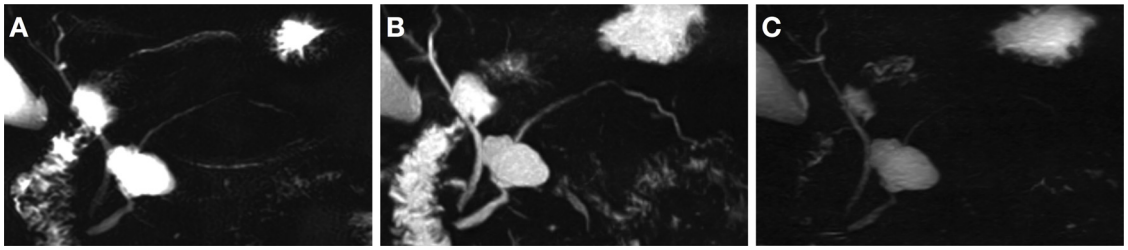

Fig. 2. Patient with a branch-duct IPMN in the pancreatic head. In this patient RT-CS10 (B) outperforms the other sequences in the depiction of the pancreatic duct yielding substantially higher signal compared to 2D-SSBH (A) and BH-CS24 (C).

the only site of pathology. This is likely due to the longer acquisition enabling superior signal in the distal PBT. Our suggestions and findings are in line with current data from Zhu et al., who also found CS acquisitions to provide better visualization of small ductal structures, with respiratory triggering offering superior results in cases of limited compliance [9; 10]. However, BH-CS24 images were acquired with a larger voxel size and longer TR ($1 \times 1x2$ mm^3, TR = 2500 ms compared to $1 \times 1x1$ mm^3, TR = 1700 ms) compared to previous studies to increase SNR. We believe that this increase in SNR could be especially critical when performing such a study in patients with larger abdominal circumference and when a larger FOV is required.

Two recent publications report on single breath hold 3D gradient and spin echo (GraSE) MRCP [18,19]. Both authors noted fewer artifacts and overall fewer non-diagnostic exams compared to conventional RT 3D MRCP. One author found small ductal structures less well visualized by the BH sequence due to lower CNR. Based on reported voxel sizes, breath hold times (up to 20 s with $1.6 \times 1.52 \times 2.0$ mm^3 voxel size) and the known sensitivity of GraSE to off-resonance effects, the proposed BH-CS24 (17 s, $1.0 \times 1.0 \times 2.0$ mm^3) sequence allows higher resolution imaging with reduced sensitivity to off-resonance effects.

Our study has limitations, most importantly a retrospective single institution study design and a limited sample size of 53 patients. Although we did not perform comparisons between BH and RT sequences acquired with and without CS; we expect the difference to be minimal as previously described [17,20]. Furthermore, we compared a 2D-acquisition with 3D-acquisitions. Besides overall less signal, overlap of anatomical structures might thus have also contributed to lower ratings regarding visualization of smaller ductal structures in 2D-SSBH. *Line profile* analysis should also be interpreted mindful of the fact that the signal in the CBD represents summation in the 2D sequence, leading to the observed higher signal variance in 2D-SSBH. However, from a clinical standpoint inclusion of the 2D-SSBH sequence enabled us to suggest an improved workflow in patient care, seeing as single-shot 2D MRCP is still widely employed as the standard sequence. Our results might not be generalizable to all MRI systems. Taron et al. recently stated that significant differences in image quality between RT and BH acquisitions can only be observed on 3 T systems [12]. Furthermore, image quality is dependent upon the MRI system vendor, with differences having been demonstrated in previous works [20]. We did not perform correlation with concrete pathology, since we aimed at primarily comparing technical performance and documenting our initial experiences with the different sequences. The results of our study should be expanded upon with validation in specific diseases of the pancreatobiliary tree.

In conclusion, BH-CS24 allows a sub-30 s acquisition of a full, diagnostic quality 3D dataset of the pancreaticobiliary tree on latest-generation 3 T MRI systems, and thus can be regarded as the sequence of choice in patients able to comply with a 17 s breath hold.

Because MRCP is an exam that is often considered as an initial work up at our institution, we have instated BH-CS24 as the primary MRCP sequence and we do not perform further sequences if image quality is satisfactory and pathology can be ruled out. When patients cannot perform a 17 s breath hold and when small ductal structures are the primary focus, RT-CS10 can improve diagnostic confidence. The diagnostic accuracy of BH-CS24 and RT-CS10 should be evaluated systematically in future imaging studies.

Guarantor

The scientific guarantor of this publication is Rickmer Braren.

Conflict of interest

The authors acknowledge research support from Philips Healthcare

Funding

The authors state that this work has not received any funding.

Statistics and biometry

No complex statistical methods were necessary for this paper.

Informed consent

The requirement for written informed consent was waived by the institutional ethics committee.

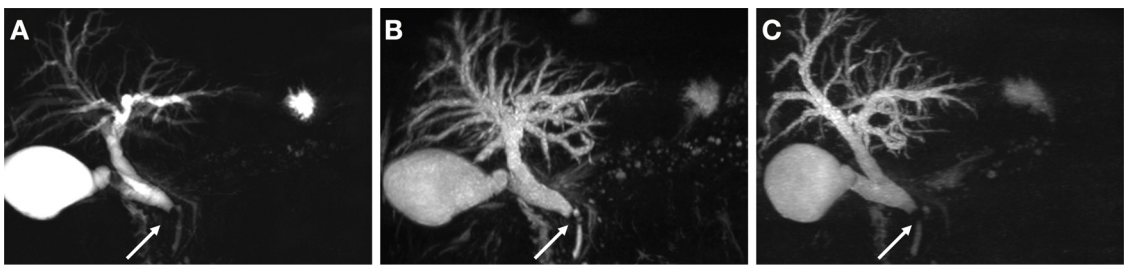

Fig. 3. Patient with a stone in the common bile duct (white arrow) and multiple small cystic pancreatic lesions. Contrast and visualization of small cystic pancreatic lesions are best in RT-CS10 (B), followed by BH-CS24 (C) and 2D-SSBH (A) However, more motion blurring is apparent in small ductal structures in RT-CS10.

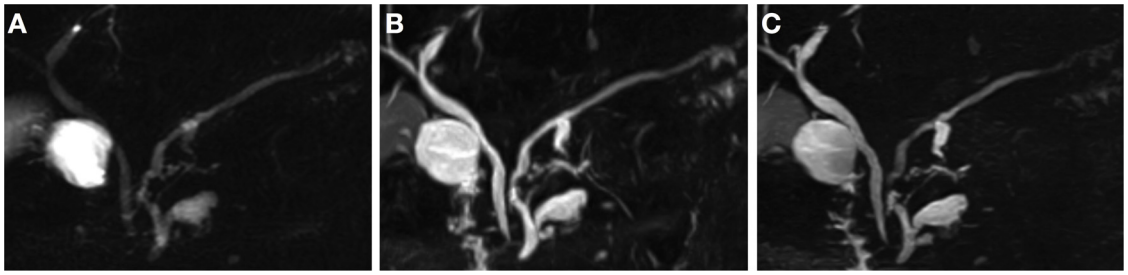

Fig. 4. Patient with a branch duct IPMN in the pancreatic head. BH-CS24 yields the sharpest image impression compared to RT-CS10 (B), which shows more blurring, and 2D-SSBH (A).

Ethical approval

Institutional Review Board approval was obtained.

Study subjects or cohorts overlap

N.A.

Methodology

- retrospective
- case-control study
- performed at one institution

References

[1] S.A. Anupindi, T. Victoria, Magnetic resonance cholangiopancreatography: techniques and applications, Magn. Reson. Imaging Clin. N. Am. 16 (2008) 453–466.
[2] M.A. Barish, E.K. Yucel, J.T. Ferrucci, Magnetic resonance cholangiopancreatography, N. Engl. J. Med. 341 (1999) 258–264.
[3] K. Liu, P. Xie, W. Peng, Z. Zhou, Magnetic resonance cholangiopancreatography: comparison of two- and three-dimensional sequences for the assessment of pancreatic cystic lesions, Oncol. Lett. 9 (2015) 1917–1921.
[4] M. Cova, F. Stacul, G. Cester, M. Ukmar, R. Pozzi Mucelli, [MR cholangiopancreatography: comparison of 2D single-shot fast spin-echo and 3D fast spin-echo sequences], Radiol. Med. 106 (2003) 178–190.
[5] K.P. Pruessmann, M. Weiger, M.B. Scheidegger, P. Boesiger, SENSE: sensitivity encoding for fast MRI, Magn. Reson. Med. 42 (1999) 952–962.
[6] M. Lustig, S.J. Kim, J.M. Pauly, A fast method for designing time-optimal gradient waveforms for arbitrary k-space trajectories, IEEE Trans. Med. Imaging 27 (2008) 866–873.
[7] T. Sartoretti, C. Reischauer, E. Sartoretti, C. Binkert, A. Najafi, S. Sartoretti-Schefer, Common artefacts encountered on images acquired with combined compressed sensing and SENSE, Insights Imaging 9 (2018) 1107–1115.
[8] L. Feng, T. Benkert, K.T. Block, D.K. Sodickson, R. Otazo, H. Chandarana, Compressed sensing for body MRI, J. Magn. Reson. Imaging 45 (2017) 966–987.
[9] L. Zhu, X. Wu, Z. Sun, et al., Compressed-sensing accelerated 3-Dimensional magnetic resonance cholangiopancreatography: application in suspected pancreatic diseases, Invest. Radiol. 53 (2018) 150–157.
[10] L. Zhu, H. Xue, Z. Sun, et al., Modified breath-hold compressed-sensing 3D MR cholangiopancreatography with a small field-of-view and high resolution acquisition: clinical feasibility in biliary and pancreatic disorders, J. Magn. Reson. Imaging 48 (2018) 1389–1399.
[11] A. Furlan, E. Bayram, S. Thangasamy, D. Barley, A. Dasyam, Application of compressed sensing to 3D magnetic resonance cholangiopancreatography for the evaluation of pancreatic cystic lesions, Magn. Reson. Imaging 52 (2018) 131–136.
[12] J. Taron, J. Weiss, M. Notohamiprodjo, et al., Acceleration of magnetic resonance cholangiopancreatography using compressed sensing at 1.5 and 3 t: a clinical feasibility study, Invest. Radiol. 53 (2018) 681–688.
[13] H. Chandarana, A.M. Doshi, A. Shanbhogue, et al., Three-dimensional MR Cholangiopancreatography in a breath hold with sparsity-based reconstruction of highly undersampled data, Radiology 280 (2016) 585–594.
[14] J.H. Yoon, S.M. Lee, H.J. Kang, et al., Clinical feasibility of 3-Dimensional magnetic resonance cholangiopancreatography using compressed sensing: comparison of image quality and diagnostic performance, Invest. Radiol. 52 (2017) 612–619.
[15] J. Schindelin, I. Arganda-Carreras, E. Frise, et al., Fiji: an open-source platform for biological-image analysis, Nat. Methods 9 (2012) 676–682.
[16] H. Kwon, S. Reid, D. Kim, S. Lee, J. Cho, J. Oh, Diagnosing common bile duct obstruction: comparison of image quality and diagnostic performance of three-dimensional magnetic resonance cholangiopancreatography with and without compressed sensing, Abdom. Radiol. (NY) 43 (2018) 2255–2261.
[17] S. Nagata, S. Goshima, Y. Noda, et al., Magnetic resonance cholangiopancreatography using optimized integrated combination with parallel imaging and compressed sensing technique, Abdom. Radiol. (NY) (2019), https://doi.org/10.1007/s00261-018-01886-0.
[18] J.G. Nam, J.M. Lee, H.J. Kang, et al., GRASE Revisited: breath-hold three-dimensional (3D) magnetic resonance cholangiopancreatography using a Gradient and spin Echo (GRASE) technique at 3T, Eur. Radiol. 28 (2018) 3721–3728.
[19] M. Yoshida, T. Nakaura, T. Inoue, et al., Magnetic resonance cholangiopancreatography with GRASE sequence at 3.0T: does it improve image quality and acquisition time as compared with 3D TSE? Eur. Radiol. 28 (2018) 2436–2443.
[20] N. Seo, et al., Feasibility of 3D navigator-triggered magnetic resonance cholangiopancreatography with combined parallel imaging and compressed sensing reconstruction at 3T, J. Magn. Reson. Imaging 46 (5) (2017) 1289–1297.